A large-depth-of-field projected fringe profilometry using supercontinuum light illumination

Wei-Hung Su*, Kebin Shi, Zhiwen Liu, Bo Wang, Karl Reichard+, and Shizhuo Yin

**Department of Material Science and Optoelectronic Engineering,*
National Sun Yat-Sen University
Kaohsiung 804, Taiwan

Department of Electrical Engineering
The Pennsylvania State University
University Park, PA 16802

+ Applied Research Lab, Penn State University
sxy105@psu.edu

Abstract: In this paper, a large-depth-of-field projected fringe profilometry using a supercontinuum light source generated by launching femto second laser pulses into a highly nonlinear photonic crystal fiber is presented. Since the supercontinuum light has high spatial coherence and a broad spectral range (from UV to near infrared), a high power (hundreds of mW) point white light source can be employed to generate modulated fringe patterns, which offers following major advantages: (1) large-depth-of-field, (2) ease of calibration, and (3) little speckle noise (a major problem for the laser system). Thus, a highly accurate, large-depth-of-field projected fringe profilometer can be realized. Both the theoretical description and experimental demonstration are provided.

OCIS codes: (120.4630) Optical inspection; (110.6880) Three-dimensional image acquisition

References and links

1. K. A. Haines, B. P. Hildebrand, "Contour generation by wavefront reconstruction," Phys. Lett. **19**, 10-11 (1965).
2. M. Takeda, K. Muta, "Fourier transform profilometry for the automatic measurement of 3-D object shaped," Appl. Opt. **24**, 3977-3982 (1983).
3. K. Creath, "Phase-measurement interferometry techniques," Prog. Opt. **26**, 350-393 (1988).
4. V. Srinivasan, H. C. Liu, and M. Halioua, "Automated phase-measuring profilometry of 3-D diffuse objects," Appl. Opt. **23**, 3105-3108 (1984).
5. V. Srinivasan, H. C. Liu, and M. Halioua, "Automated phase-measuring profilometry: a phase mapping approach," Appl. Opt. **24**, 185-188 (1985).
6. V. Y. Su, G von Bally, and D. Vukicevic, "Phase-stepping grating profilometry: utilization of intensity modulation analysis in complex objects evaluation," Opt. Commun. **98**, 141-150 (1993).
7. G. W. Lu, S. D. Wu, N. Palmer, and H. Y. Liu, "Application of phase-shift optical triangulation to precision gear gauging," Proc. SPIE **3520**, 52-63 (1998).
8. H. Y. Liu, W. H. Su, K. Reichard, and S. Yin, "Calibration-based phase-shifting projected fringe profilometry for accurate absolute 3D surface profile measurement," Opt. Comm. **216**, 65-80 (2003).
9. W. H. Su, H. Y. Liu, K. Reichard, S. Yin, and Francis T. S. Yu, "Fabrication of digital sinusoidal gratings and precisely conytolled diffusive flats and their application to highly accurate projected fringe profilometry," Opt. Eng. **42**, 1730-1740 (2003).
10. K. G. Larkin and B. F. Oreb, "Design and assessment of symmetrical phase-shifting algorithms," J. Opt. Soc. Am. A **9**, 1740-1748 (1992).
11. Y. Surrel, "Phase stepping: a new self-calibrating algorithm," Appl. Opt. **32**, 3598-3600 (1993).

#6206 - $15.00 US Received 5 January 2005; revised 31 January 2005; accepted 31 January 2005

12. W. H. Su, K. Reichard, H. Y. Liu, and S. Yin, "Integration of segmented 3D profiles measured by calibration-based phase-shifting projected fringe profilometry (PSPFP)," Opt. Mem. Neural Net. **12**, (2003).
13. T. A. Birks, J. C. Knight, and P. St. J. Russell, "Endlessly single-mode photonic crystal fiber," Opt. Lett. **22**, 961-963 (1997).
14. M. Seefeldt, A. Heuer, and R. Menzel, "Compact white-light source with an average output power of 2.4W and 900 nm spectral bandwidth," Opt. Commun. **216**, 199-202 (2003).
15. T. Schreiber, J. Limpert, H. Zellmer, A. Tűnnermann, K. P. Hansen, "High average power supercontinuum generation in photonic crystal fibers," Opt. Commun. **228**, 71-78 (2003).
16. K. Shi, P. Li, S. Yin, and Z. Liu, "Chromatic confocal microscopy using supercontinuum light," Opt. Express. **12**, 2096-2101 (2004).
17. K. R. Spring, M. W. Dividson, "Depth of field and Depth of focus," http://www.microscopyu.com/articles/formulas/formulasfielddepth.html.
18. M. Born and E. Wolf, *Principles of Optics* (Cambridge University Press, Seventh edition, 1999), Chap. 4. and Chap. 8.8.2.
19. J. B. Pawley etc., *Handbook of biological confocal microscopy* (New York: Plenum Press, 1990), Chap. 1.
20. Robert E. Wheeler, "Notes on view camera geometry," http://www.bobwheeler.com/photo/ViewCam.pdf , 2003.

1. Introduction

Projected fringe profilometry is one of the most effective methods to measure the 3D surface profiles of rough engineering surfaces [1-3]. The entire surface can be sampled simultaneously with minimum requirements on the mechanical fixture [4]. In conjunction with a phase-shifting detection scheme [5-6], depth accuracy better than one part in ten thousandths of the field of view can be achieved even with excessive image noises [7, 8]. In addition to accurate profile measurements, phase-shifting projected fringe profilometry (PSPFP) is notable for its non-contact nature, fast measurement speed, full-field measurement capability, high profile sampling density, and low environmental vulnerability [9-12].

Profile measurements by phase-shifting projected fringe methods are commonly used either in a comparative mode, in which a surface is compared to another surface and the difference is measured; or in an absolute mode, in which the depth of a single surface is measured. Both modes require a sinusoidal fringe pattern projected onto the inspected surface in order to demodulate the distorted fringe values into the corresponding depths. The depth measuring range is basically limited by the depth of field of a projection system. One possible way to extend the depth of the field is to use a laser as the projection light source. The high spatial coherence (i.e., a point source) of a laser source allows us to generate a near perfect collimated light beam. The depth of the field can be substantially increased when a collimated light beam is used to illuminate the sinusoidal fringe pattern. Furthermore, since all the light beams are originally coming from the same point, it becomes much easier to calibrate the measurement [8]. Unfortunately, coherent noise is inevitably introduced by the laser source, which is harmful to the measurement accuracy.

To maintain the advantages (i.e., large depth of the field and easiness for calibration) and eliminate the limitation (coherent noise) of the laser sources used in the projected fringe profilometry, in this paper, we investigate the use of a supercontinuum light generated by launching ultra short laser pulses into a highly nonlinear photonic crystal fibers in the projected fringe profilometry [13-16]. The ultra high spatial coherence and low temporal coherence (ultra wide spectral range from UV to near infrared) make it possible generate a nearly perfect temporally incoherent point light source. It is found that a highly accurate projected fringe profilometer can be built by applying the supercontinuum light in the system.

#6206 - $15.00 US Received 5 January 2005; revised 31 January 2005; accepted 31 January 2005

2. Depth of field under supercontinuum light illumination

In an imaging system, the total depth of field (DOF), DOF_{tot} is determined by the sum of wave (diffraction-limited), DOF_w, and geometrical optics, DOF_g, depths of field, which is mathematically expressed as [17]

$$DOF_{tot} = DOF_w + DOF_g \tag{1}$$

The diffraction-limited depth of field shrinks inversely with the square of the numerical aperture, NA, as given by [18]

$$DOF_w = k_1 \frac{\lambda}{NA^2} \tag{2}$$

where k_1 denotes a constant ($k_1 = 0.5$ for the incoherent illumination and $k_1 \approx 1$ for the coherent illumination [19]) and λ is the wavelength of illuminating light. Note that since the period of the projected fringe is usually in the millimeter order and the numerical aperture of the projection system can be very small without losing illumination efficiency via spatially coherent light illumination, DOF_w can be very large.

The geometric optics depth of field is related to the circles of confusion, which can be mathematically derived from lens equation [18, 20],

$$\frac{1}{u} + \frac{1}{v} = \frac{1}{f} \tag{3}$$

where u is in objective space and v is in image space, f is focal length of the lens. When we consider a circle of confusion with diameter c in the image space, near DOF distance and far DOF distance in objective space can be easily derived by the geometry shown in Figs. 1(a) and 1(b).

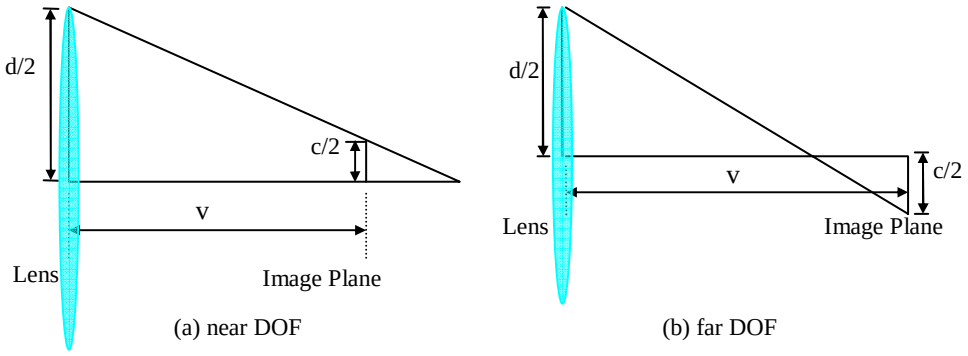

Fig. 1. Geometrical illustration of depth of field.

where d is the aperture (diameter) of the lens. The corresponding near DOF distance L_n and far DOF distance L_f are,

$$L_n = \frac{uf^2}{f^2 + (u - f)Fc} \tag{4a}$$

$$L_f = \frac{uf^2}{f^2 - (u - f)Fc}, \text{ for } f^2 - (u - f)Fc > 0 \tag{4b}$$

$$L_f = \infty, \quad \text{for } f^2 - (u - f)Fc \le 0 \tag{4c}$$

#6206 - $15.00 US Received 5 January 2005; revised 31 January 2005; accepted 31 January 2005

where F represents the f-number of an imaging system, which is equal to f/d. In Eqs. (4b) and (4c), another expression for $f^2-(u-f)Fc\le 0$ is $u\ge f(1+d/c)$. Typically d/c is a very large number. Therefore in order to obtain a large L_f at a conventional imaging system, a large u should be achieved firstly.

The total DOF then is given as,

$$L_{DOF}=L_f-L_n=\frac{2uf^2(u-f)Fc}{f^4-(u-f)^2F^2c^2},\quad \text{for } f^2-(u-f)Fc>0 \tag{5a}$$

$$L_{DOF}=\infty,\qquad \text{for } f^2-(u-f)Fc\le 0 \tag{5b}$$

define magnification $m=v/u$, equation (5) can be rewrote as,

$$L_{DOF}=\frac{2Fc\dfrac{m+1}{m^2}}{1-\chi},\qquad \text{for } \chi<1 \tag{6a}$$

$$L_{DOF}=\infty,\qquad \text{for } \chi\ge 1 \tag{6b}$$

$$\text{Where } \chi=\left(\frac{c}{md}\right)^2 \tag{6c}$$

In the projected fringe profilometry, c is determined by the period of projected fringe, T (e.g., $c=0.1T$). For example, if T is in the order of millimeter c can be in the order of sub-millimeter (e.g., 0.1 mm). Since the supercontinuum light (generated by launching the ultra short laser pulses in a highly nonlinear photonic crystal fiber) is a highly spatially coherent light source, the effective aperture of the imaging system, d, can be very small without losing light illuminating efficiency. If $md<<c$, based on Eq. (6c), $\chi\ge 1$ and a very large depth of focus (at least, under geometric optics approximation) can be obtained as given by Eq. (6b). In addition, since a well collimated illuminating beam can be generated by this supercontinuum light source, the projection imaging system can have a very small NA without losing overall illuminating efficiency. Then, based on Eq. (2), a large DOF_w can be achieved. Thus, the overall DOF of the system, DOF_T, is large.

We stress that although both the laser and the supercontinuum light are highly spatially coherent light sources, the narrow-band laser light is also a temporally coherent light source that inherently has the coherent noise, which is detrimental to the accuracy of the projected fringe profilometry. Thus, the supercontinuum light is a much better choice in the projected fringe profilometry, which has the advantages of both large depth of field and low noise.

To verify the aforementioned theory (i.e., a spatially coherent light source can offer a larger depth of field in the projected fringe profilometry), a simple imaging experiment was performed. A tilted cylindrical tube was used as the testing object. A sinusoidal pattern was projected onto the cylindrical tube using a standard imaging system as shown in Fig. 2. Figures 3(a), 3(b), and 3(c) show the recorded pictures of projected fringes under the illuminations of laser, spatially incoherent white light, and supercontinuum light sources, respectively. First, these experimental results confirmed that both the laser and the supercontinuum light sources offered a better depth of field than that of conventional spatially incoherent white light source. Furthermore, higher imaging quality was obtained by the supercontinuum light imaging system due to the lack of coherent noise.

#6206 - $15.00 US Received 5 January 2005; revised 31 January 2005; accepted 31 January 2005

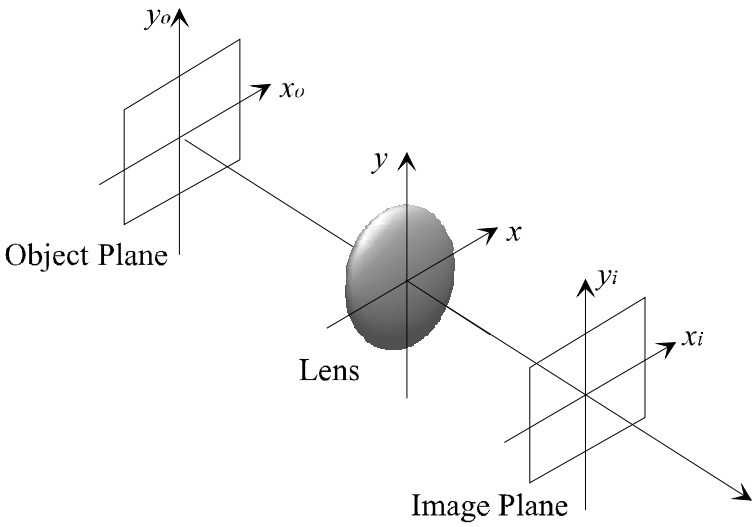

Fig. 2. Schematic diagram of a standard projection imaging system.

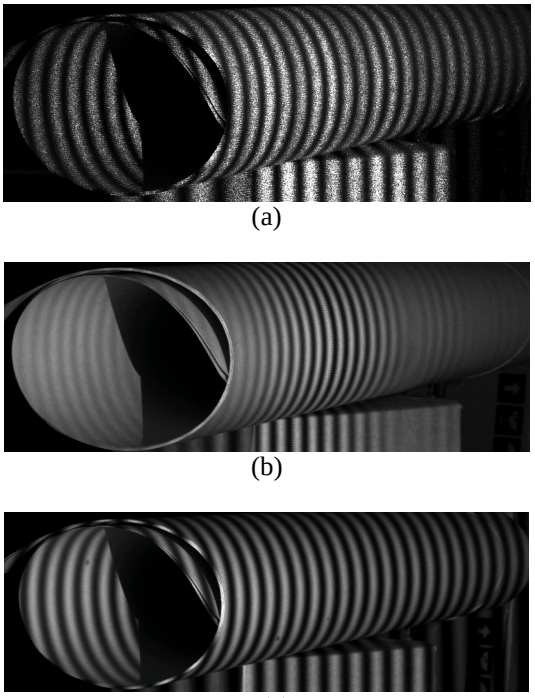

(a)

(b)

(c)

Fig. 3. Appearance of projected fringes on a tested object using different types of illumination source: (a) a laser source; (b) an extended white light source; and (c) a point supercontinuum light source.

3. Projected fringe profilometry using supercontinuum light illumination.

To study the projected fringe profilometry using the supercontinuum light illumination, a standard phase-shifting projected fringe system was built, as shown in Fig. 4, which were mainly composed of (1) a highly nonlinear photonic crystal fiber, (2) a collimating lens, (3) a

#6206 - $15.00 US Received 5 January 2005; revised 31 January 2005; accepted 31 January 2005

sinusoidal fringe pattern set on the top of a moving stage, (4) a projecting lens based imaging system, (5) a testing object, and (6) a CCD camera system used to record the projected fringes on the testing object.

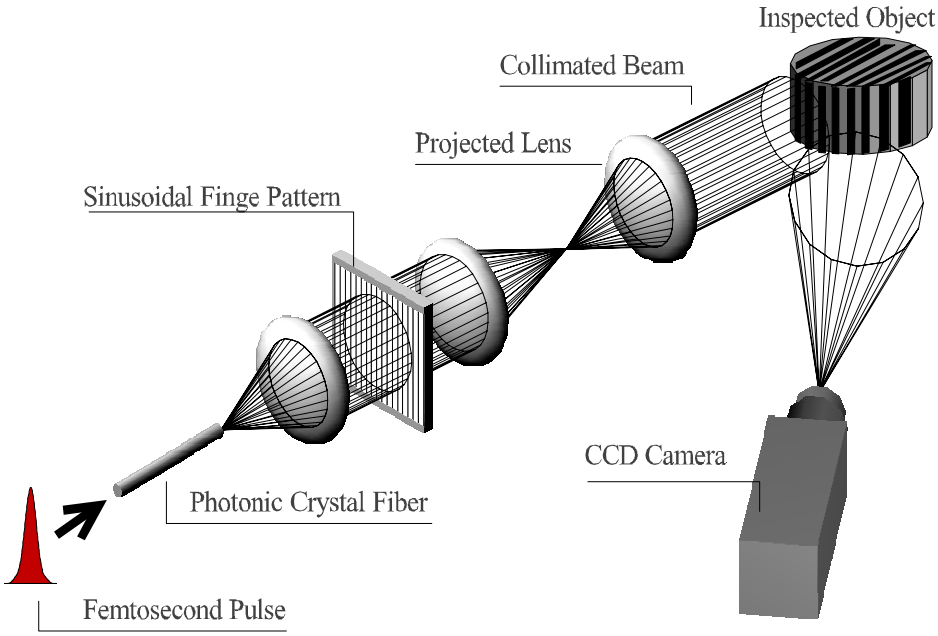

Fig. 4. Schematic diagram of a phase-shifting projected fringe profilometric system using the supercontinuum light illumination

In the experiment, the supercontinuum light was generated by launching femtosecond pusles from a mode locked Ti: Sapphire laser into a highly nonlinear photonic crystal fiber (manufactured by Crystal Fibre, model number: NL-2.0-770) [16]. Since the effective area of this fiber was very small (around 1 micron in diameter), the supercontinuum light can be generated within this short (around 10 cm) photonic crystal fiber via several nonlinear effects, including four wave mixing and Raman scattering. At the output end of the fiber, a nearly perfect white light point source was obtained. The light beams from this point source were collimated by a collimating lens and the collimated beams were employed to illuminate a sinusoidal fringe pattern. Then, the sinusoidal fringe pattern was projected onto the surface of the testing object. Finally, a CCD camera system was used to record the projected fringes on the testing object.

To measure the 3D surface profile, a standard four-step phase shifting method was utilized [7]. Four projected fringe patterns, $I_o(c,r)$, $I_1(c,r)$, $I_2(c,r)$, and $I_3(c,r)$ with a $\pi/2$ phase shifting step between adjacent patterns were recorded by the CCD camera system, as given by

$$I_0(c,r) = a(c,r) + b(c,r)\cos\left[\frac{2\pi c}{d} + \phi(c,r)\right], \tag{7a}$$

$$I_1(c,r) = a(c,r) + b(c,r)\cos\left[\frac{2\pi c}{d} + \phi(c,r) + \frac{\pi}{2}\right], \tag{7b}$$

$$I_2(c,r) = a(c,r) + b(c,r)\cos\left[\frac{2\pi c}{d} + \phi(c,r) + \pi\right], \tag{7c}$$

#6206 - $15.00 US Received 5 January 2005; revised 31 January 2005; accepted 31 January 2005

$$I_3(c,r) = a(c,r) + b(c,r)\cos\left[\frac{2\pi c}{d} + \phi(c,r) + \frac{3\pi}{2}\right], \tag{7d}$$

Where d was the nominal period of the fringes, $a(c,r)$ was the intensity bias, $b(c,r)$ was the fringe modulation at location (c,r) in the CCD detection plane, and $\phi(c,r)$ was the phase term that denoted the fringe deformation induced by the variations in the surface relief. From Eqs. 7(a) – 7(d), the phase term $\phi(c,r)$ can be derived as

$$\phi(c,r) = \arctan\left[\frac{I_3(c,r) - I_1(c,r)}{I_0(c,r) - I_2(c,r)}\right] - \frac{2\pi c}{d}. \tag{8}$$

Finally, the depth (or height) information of the 3D surface could be calculated from $\phi(c,r)$ via optical triangulation method. For example, the depth between reference points A and C, H_{AC}, can be calculated by the following equation [7]

$$H_{AC} = AC\tan\theta_0 = \frac{(\varphi_C - \varphi_A)d_0\tan\theta_0}{2\pi} \tag{9}$$

Where φ_A and φ_C are the phase values at the reference points A and C, respectively; and θ_o is the angle between the direction of the projecting light beam and the normal direction of the reference plane.

As an experimental example, a fan blade was selected as the testing object. Fig. 5 showed the fringes projected on this fan blade by the supercontinuum light illumination. One can clearly see that nice fringe patterns are obtained across the entire fan blade surface regardless of their depths. Therefore, one can indeed get a large depth of field via the supercontinuum illumination. After recording four phase-shifting fringes, the 3D surface profile of the fan blade was calculated by using Eqs. (8) and (9). Fig. 6 showed the measured 3D surface profile of the fan blade. This experimental result demonstrated that the quality of the measure was very high. There were no noticeable errors on this measurement. This measurement result was also compared with the data obtained from the standard scanning stylus surface profiler. Two measurement results agreed very well (in the micron range accuracy).

Besides the large depth of field, we also would like to point out that, due to the point light source nature of the supercontinuum light, all the projected light beams can be traced back from the same illuminating point, which makes the calibration process much easier [8]. There is no need to calibrate the perspective distortion in this case.

#6206 - $15.00 US Received 5 January 2005; revised 31 January 2005; accepted 31 January 2005

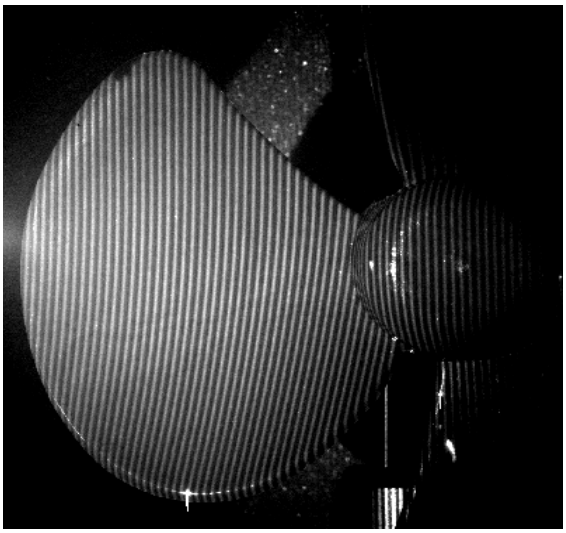

Fig. 5. Fringes projected on a fan blade via supercontinuum light illumination.

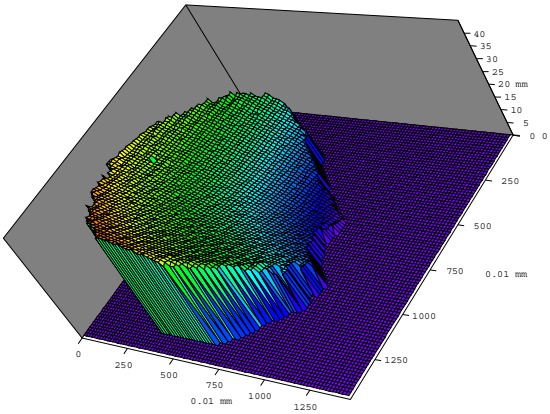

Fig. 6. Measured 3D surface profile of a fan blade

4. Conclusion

In summary, we investigated a unique projected fringe profilometry based on the supercontinuum light illumination. First, the depth of field of the projection imaging system was analyzed. It was found that a large depth of field could be obtained by the point light source illumination. Second, the advantages of using the supercontinuum light illumination in the projected fringe profilometric system were discussed, including (1) a large depth of field, (2) easiness with calibration, and (3) no coherent noise. Finally, the theoretically predicted advantages of using the supercontinuum light illumination were experimentally confirmed. A fan blade was chosen as a testing object. The 3D surface profile of the fan blade was precisely measured across the entire surface of the fan blade. There were no noticeable errors at any location of the fan blade, regardless of its depth. We believe that a robust, highly accurate projected fringe profilometry can be realized by using the supercontinuum light illumination, which may have a variety of applications such as rough 3D surface measurement.

#6206 - $15.00 US Received 5 January 2005; revised 31 January 2005; accepted 31 January 2005